

ARTICLE OPEN



The effects of bipolar disorder granule cell hyperexcitability and lithium therapy on pattern separation in a computational model of the dentate gyrus

Selena Singh ¹, Anouar Khayachi ², Shani Stern ³, Thomas Trappenberg⁴, Martin Alda ^{5,6} and Abraham Nunes ^{4,5}✉

© The Author(s) 2025

Induced pluripotent stem cell (iPSC) derived hippocampal dentate granule cell-like neurons from individuals with bipolar disorder (BD) are hyperexcitable and more spontaneously active relative to healthy control (HC) neurons. Furthermore, these abnormalities are normalised after the application of lithium in neurons derived from clinical lithium responders (LR) only. How these abnormalities impact hippocampal microcircuit computation is not understood. We aimed to investigate the impacts of BD-associated abnormal granule cell (GC) activity on pattern separation (PS) using a computational model of the dentate gyrus. We used parameter optimization to fit the parameters of biophysically realistic granule cell (GC) models to electrophysiological data from iPSC GCs from patients with BD. These cellular models were incorporated into dentate gyrus networks to assess impacts on PS using an adapted spatiotemporal task. Relationships between BD, lithium and spontaneous activity were analysed using a linear mixed-effects model. Lithium and BD negatively impacted PS, consistent with clinical reports of cognitive slowing and memory impairment during lithium therapy. By normalising spontaneous activity levels, lithium improved PS performance in LRs only. Improvements in PS after lithium therapy in LRs may therefore be attributable to the normalisation of spontaneous activity levels, rather than reductions in GC intrinsic excitability as we hypothesised. Our results mirror previous research demonstrating that mnemonic discrimination improves after lithium therapy in lithium responders only, supporting a hypothesised link between behavioural mnemonic discrimination and dentate gyrus PS. Our work can be expanded to also consider the effects of lithium-induced neurogenesis on PS.

Translational Psychiatry (2025)15:385; <https://doi.org/10.1038/s41398-025-03559-1>

INTRODUCTION

Bipolar disorder (BD) is a mood disorder with unknown aetiology characterised by recurrent episodes of mania and depression [1], and cognitive impairments that are functionally impactful [2, 3] which persist during euthymia [4]. Both memory encoding and retrieval processes for verbal material are impacted [5–7], and additional studies link BD with poor autobiographical memory specificity [8–10] and recognition memory deficits [11, 12]. Identifying the neural mechanisms of neurocognitive impairment may inform treatment development and reduce disease burden.

The hippocampus is important for both memory and emotion, and may be involved in the pathogenesis of BD. The hippocampus is critical for encoding complex associative and autobiographical memories [13–15], and is ideally suited to promote contextually appropriate responses due to its connectivity with brain systems involved in executive functioning, motivation, stress response, and emotion [16, 17]. Recent theories have proposed that the hippocampus integrates amygdalar and prefrontal inputs to create temporal context-dependent representations that may constrain emotional responses to their appropriate contexts,

protecting against psychopathology [17]. Disruptions in hippocampal function will therefore impact memory *and* downstream emotion and cognitive processes by influencing dynamics within cortico-limbic-subcortical circuits; this dynamic hippocampal role has been proposed to play a role in BD pathogenesis [18]. Indeed, anatomical and functional imaging hippocampal abnormalities have been reported in BD.

Hippocampal abnormalities in BD include reduced hippocampal volume, reduced inhibitory interneuron expression, and an increase in recurrent excitatory projections between dentate granule cells as reported in post-mortem studies [19–21] (for review, see Frey et al. [18]). A meta-analysis of functional magnetic resonance imaging studies has reported hyperactivity in limbic (i.e., parahippocampal, hippocampal and amygdalar) areas in BD relative to healthy individuals [22]. Lithium, the gold-standard prophylactic for BD, may protect against BD-associated hippocampal volume loss [23, 24]. In summary, the hippocampus is a region of interest in BD, but the physiological abnormalities that would impact neural computation, leading to the cognitive deficits described earlier, are still unknown.

¹Department of Psychology, Neuroscience and Behaviour, McMaster University, Hamilton, ON, Canada. ²Montreal Neurological Institute, Department of Neurology & Neurosurgery, McGill University, Montréal, QC, Canada. ³Sagol Department of Neurobiology, Faculty of Natural Sciences, University of Haifa, Haifa, Israel. ⁴Faculty of Computer Science, Dalhousie University, Halifax, NS, Canada. ⁵Department of Psychiatry, Dalhousie University, Halifax, NS, Canada. ⁶National Institute of Mental Health, Klecany, Czech Republic. ✉email: nunes@dal.ca

Received: 8 April 2024 Revised: 21 July 2025 Accepted: 18 August 2025

Published online: 07 October 2025

Induced pluripotent stem cell (iPSC) technology has recently been used to create hippocampal cell models in-vitro from stem cells derived from individuals with BD, to study the cellular physiological abnormalities of BD [25, 26]. Lithium responsive and non-responsive BD iPSC models of the pyramidal CA3 neuron and dentate granule cell (GC) have been created to date, and these neurons indeed have abnormal physiological properties that differ between models derived from lithium responders (LR) and lithium non-responders (NR) [25–28]. Both LR and NR iPSC neurons are hyperexcitable relative to healthy controls, and this hyperexcitability is normalised after application of lithium only for neurons derived from LRs [26]. LR-BD cell models also demonstrate elevated spontaneous activity levels relative to NR-BD and healthy control models; lithium also normalises spontaneous activity levels in LR neurons [25]. In other words, response to lithium at the cellular level corresponds to the patient's clinical response to lithium, suggesting that this cellular phenomenon may be a useful biomarker of treatment response in BD. These neurons may also play a core role in BD's pathophysiology, and explain lithium's mechanism of action. Although promising, we must acknowledge that the iPSC findings reported to date require replication in larger samples to confirm that these initial effects were not spurious. Nonetheless, how these potential abnormalities impact hippocampal microcircuit neural computation, contributing to BD-associated cognitive and memory impairments, is not yet understood.

The present study aims to investigate the impacts of GC hyperexcitability in lithium responsive and nonresponsive BD on the neural computation called *pattern separation* (PS), widely attributed to the hippocampal dentate gyrus. PS is a computation that involves mapping highly overlapping and similar inputs onto less overlapping and dissimilar outputs [29], aiding the hippocampus with encoding precise memories with minimal interference. The dentate gyrus is ideally suited to perform this computation due to the sparse, competitive firing of mature GCs that are tightly controlled by powerful inhibitory interneurons [30–32]. Supporting dentate gyrus PS, rodent studies have reported a reduction in activity correlation in the dentate gyrus relative to the entorhinal cortex and CA3 in response to slight changes in environmental stimuli [33, 34]. Independent of other circuit factors, electrophysiological [35, 36] and computational modeling [37] studies have indeed shown that GCs produce separated representations of inputs (i.e., perform PS) by shifting output spike times, highlighting both the importance of GC physiology for PS, and the GC's role in performing PS. PS within the dentate gyrus may also be behaviourally relevant, as PS has been hypothesised to underlie performance on high-interference memory tasks, such as mnemonic discrimination [38], which is a phenomenon that involves discerning between stimuli with highly overlapping qualitative properties [39]. Following this hypothesis, dentate gyrus PS deficits may therefore serve as predictors for BD-associated behavioural task performance deficits. Interestingly, results from a pilot study of mnemonic discrimination performance in BD have suggested that lithium may improve mnemonic discrimination in LRs only [40].

This work aims to predict the consequences of GC hyperexcitability on dentate gyrus PS, building a translational “bridge” between in vitro iPSC [26, 27, 41] and in vivo behavioural work [40]. We hypothesise that BD-specific GC hyperexcitability will lead to PS impairments, which will resolve after lithium-induced normalisation of hyperexcitability in LRs. We test this hypothesis by integrating detailed biophysical models of these abnormal BD GCs into a larger dentate gyrus network model, and evaluate the network's PS abilities. Our study will help elucidate neural computations underlying some of the cognitive and memory-related impairments in BD.

METHODS

To study the effects of LR and NR GC hyperexcitability, spontaneous activity, and effects of lithium on PS, we developed biophysically realistic

computational models based on empirical data from patient-derived iPSC neurons. We outline details of our approach in the Supplementary Materials, and present an intuitive description here. A schematic walkthrough of our methods is shown in Fig. 1.

Developing GC models

Ethics approval and consent to participate. All protocols were approved by the Nova Scotia Health Authority Research Ethics Board (REB # 1020604), and all participants provided informed consent.

Description of iPSC-derived dentate gyrus granule cell-like neurons. First, iPSC neurons were reprogrammed from lymphocytes and peripheral blood mononuclear cells taken from blood samples from consenting participants. Detailed methodology describing iPSC differentiation and cell culture protocols for the iPSC neurons used to inform our modelling have been previously described [41]. Briefly, blood samples were collected from 8 BD patients (4 LRs, and 4 NRs), and 5 healthy control (HC) participants (Fig. 1A). Patient ascertainment, characteristics, and assessment of lithium response are detailed in our Supplementary Materials, section 1.1.1. After lymphocyte and peripheral blood mononuclear cell isolation, followed by iPSC differentiation as described previously [26, 41], about half of the neurons per group were exposed to therapeutic levels of lithium (~1.5 mM), for 7 days. The following number of iPSC GC-like neurons per group were used for whole-cell patch-clamp recordings: LR: ($n_{Li} = 49$, $n_{CTRL} = 55$); NR: ($n_{Li} = 41$, $n_{CTRL} = 45$); HC: ($n_{Li} = 42$, $n_{CTRL} = 40$). Sodium and potassium current-voltage and frequency-current relationships were acquired in voltage-clamp and current-clamp modes respectively.

Computational model of a dentate GC. We then adapted a computational model of the hippocampal dentate GC [37, 42–44] implemented in the NEURON simulation environment (v. 8.0) [45]. This cellular model has two identical dendrites with four compartments each, and a single compartment for the soma (Fig. 1B). Distributed along the somatodendritic tree are 11 different ion-channels: fast sodium (Na), fast and slow delayed rectifier potassium, A-type potassium, large conductance calcium, voltage-dependent potassium, small conductance calcium-dependent potassium, T-type, N-type, and L-type voltage-gated calcium, inward-rectifier potassium and the tonic GABA_A chloride channel. The dynamics of each of these channels are described by sets of differential equations that are parameterized to produce behaviour consistent with real-world GCs. Together, these parameters govern the intrinsic excitability and behaviour of these model neurons. To ensure these models captured the behaviour of real-world iPSC-derived neurons from BD and HC participants, we fit these parameters using numerical optimization to the frequency-current and current voltage electrophysiological data described previously (Fig. 1B).

Numerical optimization-based fitting of computational models to cellular data. Parameter optimization was conducted using an evolutionary algorithm using the *inspyred* (v. 1.0) and *NetPyNe* (v. 1.0.0.2) Python packages. The objective function minimised was the averaged mean squared error between model and averaged iPSC-neuron FI and IV curves (for each group: HC, LR, NR), for iPSC neurons with and without exposure to lithium (“LITM” and “CTRL”, respectively). This procedure therefore generated six models: HC-CTRL, HC-LITM, LR-CTRL, LR-LITM, NR-CTRL and NR-LITM. Evolutionary algorithms perform parameter optimization by iteratively mutating, then evaluating the “fitness” of a parameter set [46]. We deemed the model fits satisfactory if each simulated data point fell within the empirical standard error of the mean.

Granule cell-like neuron models for lithium nonresponders. Experimental data failed to show a statistically significant effect of lithium exposure on frequency-current and current-voltage relationships for the NR iPSC GCs, meaning these two curves were statistically identical. Therefore, to produce a NR-LITM model, we began with the fitted NR-CTRL model and modified the parameters by increasing or decreasing their values by a random value less than 2% of the original parameter's value to introduce some noise (detailed in our Supplementary Materials, section 1.1.3). This approach yielded two models with slight differences that have comparable parameter values and biophysical behaviour, which we believe are good candidates for simulating NR-CTRL and NR-LITM conditions.

Simulation of spontaneous activity. Randomly selected GCs within the network were equipped with Poisson spike generators, synapsed onto GC

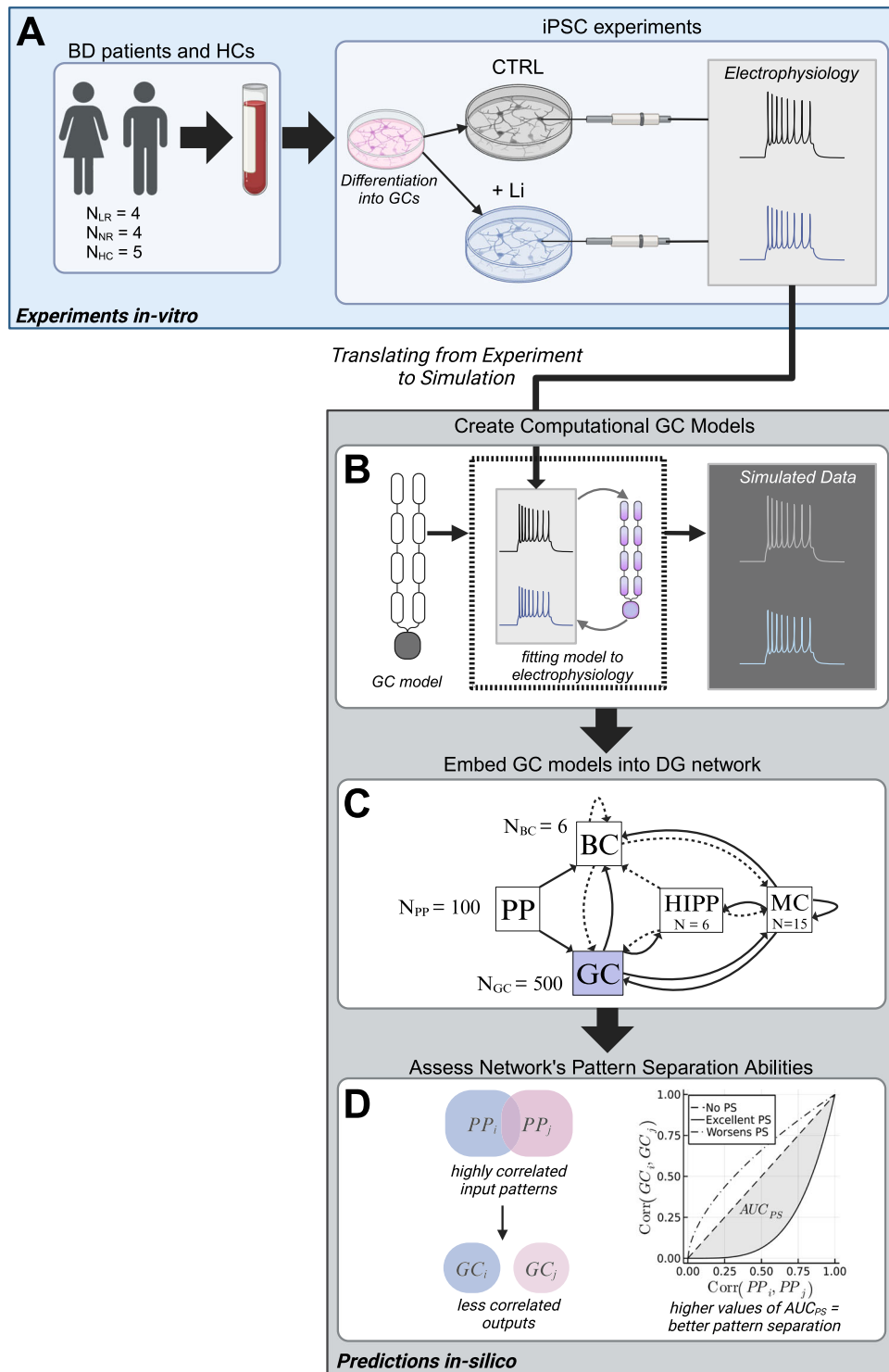


Fig. 1 Schematic of study methodology: from human participants to computational modelling. **A** Blood samples were first collected from individuals with bipolar disorder (BD) (both lithium responders, LR, and non-responders, NRs) and healthy controls (HCs), and cells were reprogrammed into granule cell (GC)-like neurons. Half of the GCs were exposed to lithium, and the electrophysiological properties of these neurons were studied. These results have been previously reported by Khayachi et al. [41]. **B** We used these electrophysiological data (frequency-current and current-voltage curves specifically) to fit the parameters of a model GC such that the model generated the same electrophysiological behaviour as the in-vitro GCs. Note: spike trains shown here are for illustrative purposes only, and are not real GC spike trains. **C** These model GCs were then incorporated into a biophysical dentate gyrus (DG) network, to form model DGs for LR, NRs and HCs. Abbreviations are as follows: PP perforant path, BC basket cell, HIPP hilar perforant path cells, MC mossy cell. Solid lines indicate excitatory connections, and dashed lines indicate inhibitory connections. N indicates the number of cells per population. This circuit diagram was adapted from our previous paper [37]. **D** The pattern separation (PS) performance of these networks were then assessed, by presenting the network with a series of partially overlapping PP input patterns, and assessing whether the resulting output patterns were less correlated. Plotting the correlation between pairs of input patterns and resulting output patterns against each other generated a PS curve. The area between the diagonal and this pattern separation curve (AUC_{PS}) summarised the network's PS abilities, with larger AUC_{PS} values representing better PS.

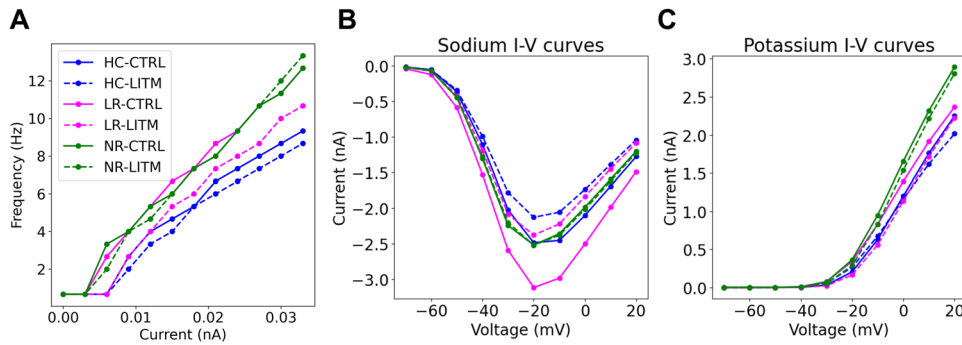


Fig. 2 Model GC electrophysiology for HC, LR and NR models, with and without lithium. **A** frequency-current relationships. BD models are more excitable than HC models, and excitability is reduced for LRs and HCs after lithium exposure (dashed lines). **B** Sodium current-voltage relationships. Lithium reduces sodium current magnitudes for LRs and HCs. **C** Potassium current-voltage relationships. NRs have greater potassium currents than LRs and HCs.

somata, randomly produced spikes at the following rates during the simulation, following previous experimental reports [25]: HC and NRs = 0.25 Hz; LRs = 1 Hz. The effect of lithium on spontaneous activity was captured by setting the LR spontaneous activity level back to HC levels of 0.25 Hz [25].

Biophysical network model of the dentate gyrus

We then incorporated the model GCs into a dentate gyrus network, to assess how BD-associated GC electrophysiological abnormalities may affect PS functioning. We employed a previously established conductance-based biophysical model of the dentate gyrus [37, 43, 44], also implemented in NEURON [45]. We preserved the original model's geometric and topological features. Our model included 500 glutamatergic GCs (as described earlier), 6 GABAergic basket cells, 15 glutamatergic mossy cells, 6 GABAergic hilar perforant path cells, and 100 excitatory entorhinal perforant path cells (Fig. 1C). As with the GCs, the basket, mossy and hilar perforant path cells were modelled as multicompartmental Hodgkin-Huxley style neurons with a soma and varying numbers of dendrites. Details regarding these neurons can be found in our Supplementary Materials. Perforant path cells were modelled as point processes that stimulated GCs and basket cells.

All biophysical properties were kept the same as in the original model [37, 43, 44]. Parameter values for the connectivity, cellular biophysics, and synaptic double-exponential functions can also be found in our Supplementary Materials, and are also described in our previous study using this model [37].

Spatiotemporal PS task. We assessed PS using a previously established spatiotemporal PS task [37, 43, 47]. 24 partially overlapping perforant path patterns, varying smoothly in degrees of overlap, were presented to the dentate gyrus at the beginning of a 200 ms simulation. We then assessed whether pairs of the resulting GC output pattern representations were less correlated than the inputs by computing Pearson correlations (Fig. 1D). By using the correlation of input patterns as x coordinates and the correlation of output representations as y coordinates, plotting this relationship between inputs and outputs should produce a curve that falls below the leading diagonal if the network performed PS (Fig. 1D). In other words, highly correlated inputs should be mapped onto less correlated outputs. We computed a summary PS index defined as the area between the leading diagonal and the PS curve (AUC_{PS}). Higher values of AUC_{PS} indicate stronger PS by the dentate gyrus network (Fig. 1D). Additional details can be found in our Supplementary Materials, section 1.2.1.

Statistical analysis

The predicted impacts of group (HC, NR, LR), treatment (with lithium and without) and spontaneous activity (baseline vs. pathological) on standardised (i.e., z -scored) PS scores (AUC_{PS}) were characterised by the following linear mixed effects model, presented here in *R* syntax for the *lme4* package in the *R* programming language [48]:

$$AUC \sim \text{Group} * \text{Lithium} * \text{SpontActiv} + (1|ID)$$

where *ID* refers to each simulation run, which is initialised with a different random seed to incorporate variability in network connectivity and which

GCs are spontaneously active. A priori power calculations using the *simR* package in *R* showed that 14 simulation runs per experimental condition offered 80% power to detect a 5% change in AUC_{PS} at a statistical significance threshold of $\alpha = 0.05$ for the three-way interaction. Model coefficients are reported as standardised effects, in the number of standard deviations of AUC_{PS} .

Assessing k winner-take-all dynamics

The competitive activation of GCs controlled by basket cell lateral inhibition promotes dentate gyrus PS. In our network, GCs are organised into lamellar clusters around basket cells, with each basket cell projecting onto 100 GCs. Under a winner-take-all paradigm, the stimulation of a few GCs should inhibit the other GCs within the lamella via these basket cell projections. This will promote the selective firing of a few GCs, or a sparse coding regime, supporting PS [32, 49–53]. To further understand the effects of BD and lithium on PS, we analysed our network's winner-take-all dynamics as follows. Each spontaneous stimulation event (described in section 2.1.6) was treated as a randomised trial. For each lamella and across the 24 patterns used in the PS analysis, we assessed the aggregate population-level behaviour of both directly stimulated non-stimulated GCs within a 10 ms window post-spontaneous stimulation. This activity was averaged across 14 simulation runs. Under a winner-take-all paradigm, we expect a peak in activity within GCs that are directly activated (these neurons are therefore the "winners"), and little to no change in behaviour within GCs that are not directly activated, suggesting tight inhibitory control, and thus a strict "selection" process, of the neurons within these lamellar microcircuits.

Cellular response to negative currents

Given that a winner-take-all mechanism for PS is dependent on the inhibition of GCs, studying GC neuronal sensitivity to inhibition is essential. For this computational protocol, current was injected into the somatic compartment for 1 s from -33–0 pA in 3 pA steps, and the overall membrane potential was recorded, mirroring the protocol used for the iPSC GCs in-vitro.

RESULTS

Fitting GC model to iPSC data

Results from our parameter fitting procedure are shown in Supplementary Fig. 2 with parameter values in Supplementary Table 5, and spike trains for each model shown in Supplementary Fig. 3. Our model fitting procedure was successful in capturing the group-level differences in cellular physiology between LR, NR and HCs (iPSC data shown in Supplementary Fig. 1), in that through parameter differences, our LR-LITM model demonstrated reduced GC hyperexcitability, and sodium and potassium current magnitudes, in contrast with the LR-CTRL and NR models (Fig. 2). We observed a similar, albeit smaller, effect in the HC-LITM model (Fig. 2).

Effects of BD hyperexcitability and lithium on PS

PS performance for dentate gyrus networks with HC and BD GC models, for baseline and pathological levels of spontaneous

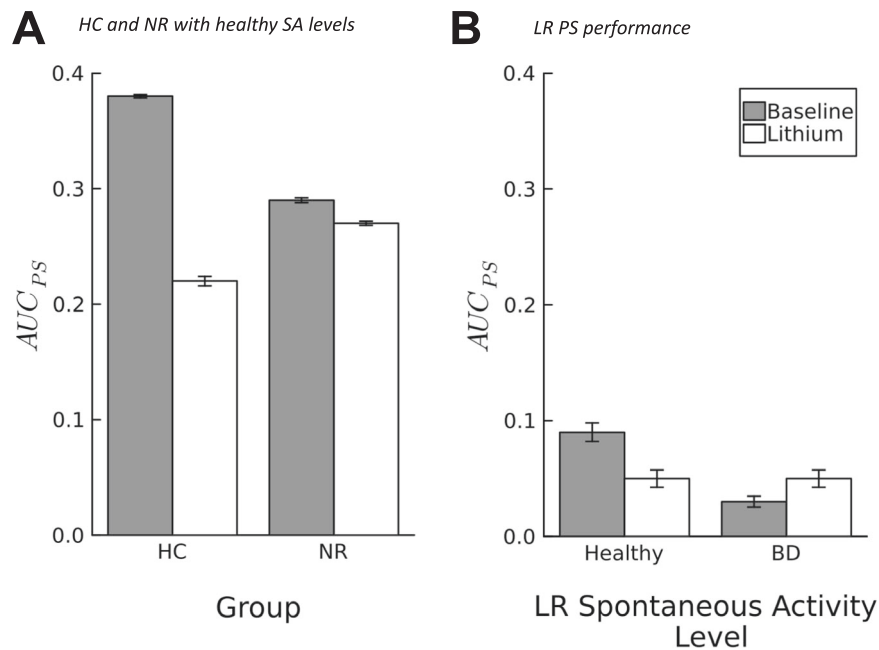


Fig. 3 Effects of BD models on pattern separation (PS). **A** Healthy levels of spontaneous activity (SA) used for HC and NR models (0.1 Hz [25]), and **B** pathological levels of spontaneous activity used for the LR condition (Healthy = 0.1 Hz; BD = 1 Hz, normalised to healthy levels after lithium exposure [25]). Error bars show standard error of the mean, for 14 simulation runs initialised with different random seeds to incorporate variability in network connectivity and granule cells selected for spontaneous activation.

activity, is shown in Fig. 3, and full statistical results from the linear mixed model analysis are presented in Supplementary Table 2. BD DG models performed significantly poorer PS than HC models, regardless of spontaneous activity levels and lithium treatment (LR: $\beta = -2.37$, CI: $-2.46 - -2.29$, $p < 0.001$; NR: $\beta = -0.75$, CI: $-0.83 - -0.66$, $p < 0.001$) (Fig. 3). Lithium, independent of *Group* or *Spontaneous Activity*, significantly and negatively impacted PS in general ($\beta = -1.32$, CI: $-1.41 - -1.24$, $p < 0.001$) (Fig. 3). Although lithium reduced the excitability of HC GCs (Fig. 2A), it also reduced HC PS performance (Fig. 3A).

Elevated spontaneous activity levels in LRs without lithium therapy negatively impacted PS (Fig. 3B) (LR x Spontaneous Activity; $\beta = -0.45$, CI: $-0.57 - -0.33$, $p < 0.001$). Lithium therapy however protected against the deleterious effects of spontaneous activity on PS for LRs (Fig. 3B) (LR x Lithium x Spontaneous Activity; $\beta = 0.39$, CI: $0.22 - 0.56$, $p < 0.001$).

Lithium disrupts winner-take-all dynamics in HCs by reducing neuronal sensitivity to negative currents

HC GC population behaviour within the third dentate gyrus lamella 10 ms post-spontaneous activation is shown in Fig. 4 for the GCs directly activated ("AC") and the remaining GCs within the lamella ("RM"). Without lithium, GC population activity increased 2 ms post-stimulation, and declined steadily for 3 ms before reaching a steady state of low activity (Fig. 4A, "CTRL-AC"). Activity within the remaining GCs did not change (Fig. 4B, "CTRL-RM"). In the lithium-exposed GC model, the directly activated GCs fired more than the CTRL condition post-stimulation, with a similar reduction and stabilisation of activity after 3 ms (Fig. 4A, "LITM-AC"); however, in the remaining (i.e., unstimulated) GCs, there was a substantial and sustained increase in population activity, indicative of activity "spillover" or insufficient inhibition (Fig. 4B, "LITM-RM"). This behaviour was consistent across lamellae, and also for the BD NR models (Supplementary Fig. 5). LR models demonstrated similar RM activity-level differences between CTRL and LITM conditions, but to a lesser degree (Supplementary Fig. 4).

At the cellular level, our lithium-exposed HC GC model demonstrated less sensitivity (i.e., reduced hyperpolarized

response) to negative currents than the control model (Fig. 4C). These results align qualitatively with electrophysiological data collected from iPSC GCs in vitro (Fig. 4D). Lithium increased sensitivity to negative currents in both our LR GC models, and in iPSC GCs in vitro (Supplementary Fig. 4).

DISCUSSION

Simulated GC hyperexcitability disrupted PS in BD models relative to HCs (Fig. 3). Given that PS within the DG is supported by the intrinsically sparse firing of mature GCs [32, 50, 54, 55], we hypothesised that increased intrinsic excitability of these neurons would lead to PS impairments, which our simulations support. We expected lithium to improve PS in the LR and HC models by reducing GC intrinsic excitability. Instead, lithium-induced reductions in GC excitability in LRs and HCs *impaired* PS relative to baseline (i.e., without lithium) models when controlling for spontaneous activity levels (Fig. 3); lithium therefore may not ameliorate PS deficits in LRs by reducing GC intrinsic excitability. Instead, lithium may protect against the loss of PS that would occur with higher spontaneous activity levels in LRs (Fig. 3B). Additionally, we identified that lithium not only reduced excitability in HCs, but also sensitivity to negative injected currents (Fig. 4C, D). This reduced sensitivity may prevent effective basket cell inhibition, leading to inappropriately elevated network activity (Fig. 4A, B), explaining why lithium impaired PS in HCs. Therefore, GC hyperexcitability in BD may lead to PS disruptions, and lithium may prevent these deficits in LRs not by normalising hyperexcitability, but by reducing spontaneous activity levels.

We simulated spontaneous activity by randomly stimulating a subset of GCs within the network using Poisson spike generators, as the cellular or network mechanism by which this spontaneous activity arises has not yet been identified. Spontaneous activity has been attributed to depolarizing GABA currents [56] and the interplay between sodium and calcium discharges [57] in developing hippocampal circuits, and is thought to tune network development and synchrony [58, 59], raising questions about the implications of elevated spontaneous activity on synaptic

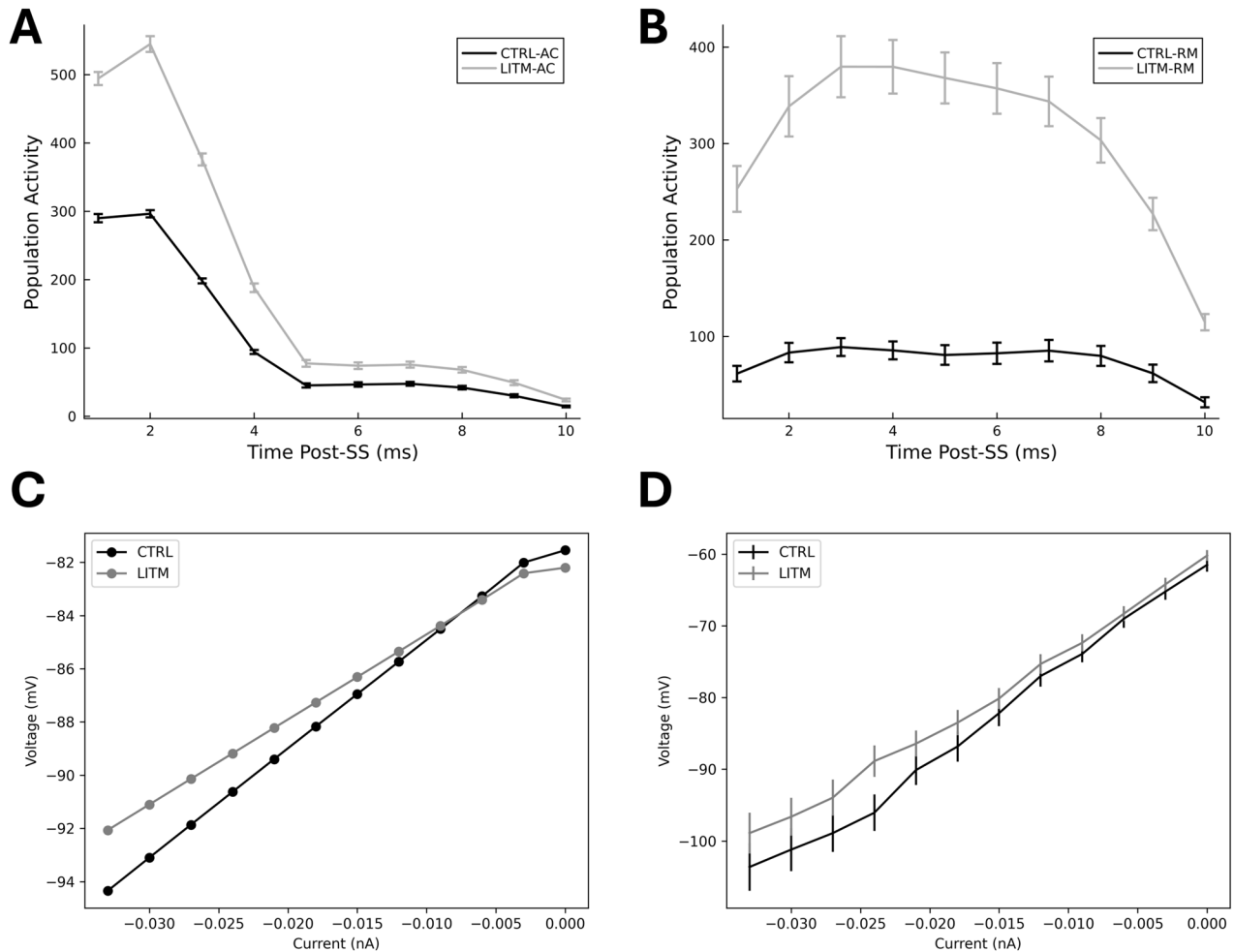


Fig. 4 Effects of lithium on healthy control winner-take-all dynamics in DG model, and cellular response to negative currents both in silico and in vitro. Winner-take-all dynamics in DG model are shown in panels **A**, **B**, and cellular response to negative currents in GC model and in-vitro are shown in panels **C**, **D** respectively. **A** GC activity after direct spontaneous stimulation (SS) (“-AC”), and **B** activity of remaining GCs not directly stimulated by spontaneous activity (“-RM”) in lamella 3 only. **C** HC-CTRL and HC-LITM GC computational model behaviour in response to negative current injection, and **D** HC-CTRL and HC-LITM iPSC GC in-vitro behaviour in response to negative current injection. Error bars show standard error of the mean.

plasticity and the functioning of memory systems in BD. Interestingly, elevated spontaneous activity within brain networks measured using fMRI may predict diagnosis conversion from major depressive disorder to BD [60], highlighting the importance of understanding spontaneous activity in BD further. Identifying the neural mechanisms of spontaneous activity observed in iPSC GCs, and whether this mechanism also exists in vivo, are worthwhile avenues for future investigation. Based on our results, we would predict that treatments aimed at reducing spontaneous activity levels in LRs may preserve PS while avoiding the potential negative effects of lithium therapy.

Indeed, lithium impaired PS for all groups when controlling for spontaneous activity levels (Fig. 3A), despite lithium-associated reductions in GC excitability in HCs and LRs, motivating the study of winner-take-all dynamics in our network. In our HC model without lithium, only the directly stimulated GCs fire post-stimulation, with no changes in activity in the remaining GC population (Fig. 4A, B), suggesting sufficient basket cell-mediated inhibition throughout the network. The elevated and sustained activity in the remaining (i.e., unstimulated) GCs in the HC-LITM model (Fig. 4B) suggests that basket cells were unable to quiet the remaining GCs in the network, or in other words, a deficit in winner-take-all dynamics. Since we did not manipulate the BCs in our network, we hypothesised that this effect may be attributable

to reductions in HC GC sensitivity to inhibition; indeed, our simulations supported this hypothesis (Fig. 4C), agreeing with in vitro behaviour of iPSC HC GCs (Fig. 4D). Supplementary Fig. 6 presents a schematic of our interpretation of these changes in winner-take-all dynamics. In summary, although reducing excitability via lithium exposure is theoretically beneficial for neural computations that are reliant on sparse coding such as PS, the effects of lithium on cellular response to inhibition should not be ignored, as it is excitation/inhibition *balance* within networks that will ultimately promote effective neural computation.

Our cellular and circuit-level results of lithium’s mixed (i.e., both beneficial and deleterious) effects for individuals with BD echo clinical discussions of whether lithium is neuroprotective or neurotoxic [61]. There have been reports of lithium-induced cognitive side effects such as memory impairments and a subjective sense of mental “slowness” [62], contrasted with reports of lithium *improving* cognitive functions such as processing speed and verbal learning and memory in BD [63]. Despite these mixed results, lithium is effective at preventing suicide and self-harm in individuals with mood disorders [64] and relapse in individuals with BD [65]. Our results predict that lithium may lead to memory impairments in healthy individuals, motivating a future controlled trial in this group. Finally, our simulations highlight the importance of identifying predictors of lithium response, such that

the potential risks to memory systems are mitigated in non-responders, while allowing responders to benefit from lithium therapy.

One area of promise for identifying predictors may be behavioural tasks such as mnemonic discrimination that are hypothesised to probe lower-level dentate gyrus neural computational functioning. In a previous study, we hypothesised that PS may underlie mnemonic discrimination performance [37], based on two lines of evidence for the dentate gyrus's involvement (1) during mnemonic discrimination [38, 66], and (2) in PS [33, 34]. Interestingly, a pilot study of the effects of lithium therapy in BD on mnemonic discrimination performance demonstrated that lithium therapy significantly improved mnemonic discrimination performance in LR only [40]. Our simulations predict that these mnemonic discrimination improvements in LR may be attributable to lithium-induced reductions in spontaneous activity. We make this statement speculatively, given that (1) a direct empirical demonstration that PS underlies mnemonic discrimination has yet to be reported, and (2) the results from our PS simulations must be validated in vivo. Further, lithium has been demonstrated to increase hippocampal neurogenesis [67, 68], which has also been shown to improve mnemonic discrimination [69–71]. Whether lithium-induced mnemonic discrimination improvements are attributable to improvements in PS, increased neurogenesis, or some combination of the two is another avenue for future work, which we discuss further below. Future lines of research addressing these questions will contribute to our understanding of how cellular behaviour impacts neural computation, and how those impacts then translate to behaviour. Forming these mechanistic links across levels of biological hierarchy will allow for the translation of identified cellular-level deficits and drug response to potential mechanistic deficits underlying disease aetiology, observable through patient behaviour.

Strengths and limitations

Model fitting procedure. Our computational models demonstrate good face and predictive validity [72]. Face validity refers to a model's ability to simulate or capture the behaviour of the system of interest [72]. Our cellular models demonstrate face validity because they are directly fit to electrophysiological behaviour of patient- and HC-derived iPSC GCs (Supplementary Fig. 2). Predictive validity assesses a model's ability to predict the effects of interventions and experimental manipulations on the underlying condition [72]. A model with strong predictive validity will be able to generate testable predictions for a set of manipulations in the form of "synthetic" data that can later be compared against real-world data. After model fitting, we assessed our models' predictive validity by comparing our models' and iPSC GCs' membrane response to negative currents (negative current-voltage curve) with and without lithium and found that our models were able to predict lithium-induced (1) reductions in sensitivity to negative currents observed in HCs (Fig. 4C, D), and (2) increases in sensitivity to negative currents observed in LR (Supplementary Fig. 4C, D), despite fitting these models to the positive current-voltage and frequency-current data only. Additionally, our simulations are consistent with the effects of lithium on mnemonic discrimination performance in individuals with BD [40]. Therefore our fitted GC models exhibit good face and predictive validity, supporting the plausibility of our simulation results.

Although our model fitting procedure was generally successful in producing the iPSC GC behaviour, we had difficulties with fitting the potassium current-voltage curves (Supplementary Fig. 2). The potassium channels for all of our computational models were, as a result, more resistant to negative currents than their iPSC counterparts. This issue may be attributable to inaccurate modelling of the potassium channel dynamics and/or a missing potassium channel; the baseline GC model used for this study

should therefore be re-visited after further genetic analysis, electrophysiology and immunohistochemistry to identify other relevant channel types, their dynamics, and their location on the somatodendritic tree. Additionally, to improve the data available for model fitting purposes, we encourage researchers to follow the electrophysiology protocols outlined by the Allen Brain Institute [73]. Overall, we do not believe that this effect would change the general result of our study as every group/condition was impacted and we were more interested in the relative differences in PS between groups/condition; instead, we believe that this limitation should be addressed in the future, to further improve model face validity.

Improving our model design. We made a number of simplifications to our model design that limit biological plausibility. The dentate gyrus is known to have a subpopulation of adult-born immature GCs that, in contrast to their mature counterparts, are highly intrinsically excitable [74], plastic [75], and are not yet regulated by inhibitory interneurons [76, 77]. Simulations have suggested that immature GCs may reduce PS but increase performance on high interference memory tasks [78], which is consistent with studies demonstrating the positive impacts of neurogenesis on discrimination performance [69–71]. As discussed previously, lithium improves mnemonic discrimination performance in LR [40], and also may upregulate neurogenesis in the dentate gyrus [67, 68]. Lithium may also reduce mossy fiber sprouting [21], and promote both axonal growth cone "spread" [79] and consequent hippocampal synaptogenesis [80]. A natural progression of the present model would be to incorporate a subpopulation of immature GCs along with the additional impacts of lithium on GC axonal growth and synaptogenesis, and subsequently evaluate PS and performance on a high interference memory task, following previous modellers [78]. This approach would therefore allow for the study of the *combined* impacts of lithium-induced (1) reductions in mature GC intrinsic excitability and spontaneous activity (as we have done here), (2) upregulated neurogenesis, (3) reduced mossy fiber sprouting, and (4) synaptogenesis on *both* PS and mnemonic discrimination, to provide us with a more comprehensive and nuanced understanding of lithium's impacts on dentate gyrus neural computation.

There have been two iPSC hippocampal neuronal models created to date: the dentate gyrus GC, and the CA3 pyramidal neuron [25–28]. Although the electrophysiological findings from iPSC studies are promising, they require replication in larger samples. Accordingly, our modelling results should be interpreted with caution, as they are contingent on the robustness of those empirical findings. Furthermore, future iPSC work should also consider other neural cell types. BD and lithium may also impact the inhibitory interneurons within the hippocampus and dentate gyrus, of which iPSC neuronal models have not yet been reported. It is pertinent to study the behaviour of the inhibitory neurons using iPSC technology as well, especially given that our simulations demonstrated that negative cellular currents modulate network dynamics and PS. Incorporating detailed models of BD inhibitory interneurons into our network will further improve biological plausibility, and allow investigation of the interplay between abnormal excitatory/inhibitory network dynamics in BD, and subsequent impacts on PS.

Since the time of earlier hippocampal computational models [50, 81], hippocampal research has revealed a number of other dentate gyrus computations along with PS, such as contextual binding, novelty detection, temporal tagging, and indexing [82]. We studied PS here as a fundamental computation that the dentate gyrus is ideally suited to perform, but also recognise that it would be beneficial for future work to investigate the impacts of BD on these other computations. PS seemingly does not conflict with these other proposed computations [82], meaning these

future results may not contradict the results we presented here, but rather add to our understanding of dentate gyrus function in BD. How those other computations then relate to behaviour, and what the clinical implications may be, are yet additional questions.

CONCLUSIONS

We presented the first detailed biophysical computational model of BD-associated GC hyperexcitability and effects of lithium therapy. We evaluated impacts of the abnormal cellular behaviour on PS using network models, and found that (1) both BD and lithium impair PS, (2) lithium may protect against the loss of PS attributable to high spontaneous activity levels in LRs, and (3) lithium reduces sensitivity to negative currents in HCs, impairing inhibitory control over GCs. Our results are consistent with clinical reports of BD and lithium-associated cognitive slowing and memory impairments, and also with a hypothesised relationship between DG PS and mnemonic discrimination. In conclusion, we presented a first step in translating abnormal iPSC-derived neuronal activity in BD to neural computational deficits that may underlie BD-related cognitive and memory impairments.

DATA AVAILABILITY

Code used for our simulations is available on ModelDB (Model 2018014).

REFERENCES

- Grande I, Berk M, Birmaher B, Vieta E. Bipolar disorder. *Lancet*. 2016;387:1561–72. [https://doi.org/10.1016/S0140-6736\(15\)00241-X](https://doi.org/10.1016/S0140-6736(15)00241-X)
- Atre-Vaidya N, Taylor MA, Seidenberg M, Reed R, Perrine A, Glick-Oberwise F, et al. Cognitive deficits, psychopathology, and psychosocial functioning in bipolar mood disorder. *Cogn Behav Neurol*. 1998;11:120.
- Sanchez-Moreno J, Martinez-Aran A, Tabarés-Seisdedos R, Torrent C, Vieta E. Functioning and disability in bipolar disorder: an extensive review. *Psychother Psychosom*. 2009;78:285–97. <https://doi.org/10.1159/000228249>
- Solé B, Jiménez E, Torrent C, Reinares M, Bonnin CdM, Torres I, et al. Cognitive impairment in bipolar disorder: treatment and prevention strategies. *Int J Neuropsychopharmacol*. 2017;20:670–80. <https://doi.org/10.1093/ijnp/pyx032>
- Bourne C, Aydemir Ö, Balanzá-Martinez V, Bora E, Brissos S, Cavanagh JTO, et al. Neuropsychological testing of cognitive impairment in euthymic bipolar disorder: an individual patient data meta-analysis. *Acta Psychiatr Scand*. 2013;128:149–62. <https://doi.org/10.1111/acps.12133>
- Kurtz MM, Gerraty RT. A meta-analytic investigation of neurocognitive deficits in bipolar illness: profile and effects of clinical state. *Neuropsychology*. 2009;23:551–62. <https://doi.org/10.1037/a0016277>
- Arts B, Jabben N, Krabbendam L, van Os J. Meta-analyses of cognitive functioning in euthymic bipolar patients and their first-degree relatives. *Psychol Med*. 2008;38:771–85. <https://doi.org/10.1017/S0033291707001675>
- Dempsey RC, Gooding PA, Jones SH. Assessing the specificity of autobiographical memory in individuals at a trait-based vulnerability to bipolar disorder using a sentence completion task. *Memory*. 2014;22:222–31. <https://doi.org/10.1080/09658211.2013.778289>
- Boulanger M, Lejeune A, Blairy S. Overgenerality memory style for past and future events and emotions related in bipolar disorder. What are the links with problem solving and interpersonal relationships? *Psychiatry Res*. 2013;210:863–70. <https://doi.org/10.1016/j.psychres.2013.06.029>
- Mowlds W, Shannon C, McCusker CG, Meenagh C, Robinson D, Wilson A, et al. Autobiographical memory specificity, depression, and trauma in bipolar disorder. *Br J Clin Psychol*. 2010;49:217–33. <https://doi.org/10.1348/014466509X454868>
- Getz GE, Shear PK, Strakowski SM. Facial affect recognition deficits in bipolar disorder. *J Int Neuropsychol Soc*. 2003;9:623–32. <https://doi.org/10.1017/S15355617703940021>
- Benito A, Lahera G, Herrera S, Muncharaz R, Benito G, Fernández-Liria A, et al. Deficits in recognition, identification, and discrimination of facial emotions in patients with bipolar disorder. *Braz J Psychiatry*. 2013;35:435–8. <https://doi.org/10.1590/1516-4446-2013-1086>
- Penfield W, Milner B. Memory deficit produced by bilateral lesions in the hippocampal zone. *AMA Arch Neurol Psychiatry*. 1958;79:475–97. <https://doi.org/10.1001/archneurpsyc.1958.02340050003001>
- Kirwan CB, Bayley PJ, Galván VV, Squire LR. Detailed recollection of remote autobiographical memory after damage to the medial temporal lobe. *Proc Natl Acad Sci USA*. 2008;105:2676–80. <https://doi.org/10.1073/pnas.0712155105>
- Söderlund H, Moscovitch M, Kumar N, Mandic M, Levine B. As time goes by: Hippocampal connectivity changes with remoteness of autobiographical memory retrieval. *Hippocampus*. 2012;22:670–9. <https://doi.org/10.1002/hipo.20927>
- Becker S, Wojtowicz JM. A model of hippocampal neurogenesis in memory and mood disorders. *Trends Cogn Sci*. 2007;11:70–76. <https://doi.org/10.1016/j.tics.2006.10.013>
- Wang J, Tambini A, Lapate RC. The tie that binds: temporal coding and adaptive emotion. *Trends Cogn Sci*. 2022;26:1103–18. <https://doi.org/10.1016/j.tics.2022.09.005>
- Frey BN, Andreazza AC, Nery FG, Martins MR, Quevedo J, Soares JC, et al. The role of hippocampus in the pathophysiology of bipolar disorder. *Behav Pharmacol*. 2007;18:419–30. <https://doi.org/10.1097/FBP.0b013e3282df3cde>
- Konradi C, Zimmerman EI, Yang CK, Lohmann KM, Gresch P, Pantazopoulos H, et al. Hippocampal interneurons in bipolar disorder. *Arch Gen Psychiatry*. 2010;68:340. <https://doi.org/10.1001/archgenpsychiatry.2010.175>
- Pantazopoulos H, Lange N, Baldessarini RJ, Berretta S. Parvalbumin neurons in the entorhinal cortex of subjects diagnosed with bipolar disorder or schizophrenia. *Biol Psychiatry*. 2007;61:640–52. <https://doi.org/10.1016/j.biopsych.2006.04.026>
- Dowlatshahi D, MacQueen G, Wang J-F, Chen B. Increased hippocampal subgranular Timm staining in subjects with bipolar disorder. *Neuroreport*. 2000;11:3775–8. <https://doi.org/10.1097/00001756-200011270-00036>
- Chen C-H, Suckling J, Lennox BR, Ooi C, Bullmore ET. A quantitative meta-analysis of fMRI studies in bipolar disorder. *Bipolar Disord*. 2011;13:1–15. <https://doi.org/10.1111/j.1399-5618.2011.00893.x>
- Hajek T, Kopecek M, Höschl C, Alda M. Smaller hippocampal volumes in patients with bipolar disorder are masked by exposure to lithium: a meta-analysis. *J Psychiatry Neurosci*. 2012;37:333–43. <https://doi.org/10.1503/jpn.110143>
- Hajek T, Cullis J, Novak T, Kopecek M, Höschl C, Blagdon R, et al. Hippocampal volumes in bipolar disorders: opposing effects of illness burden and lithium treatment: Hippocampus, illness burden, and lithium. *Bipolar Disord*. 2012;14:261–70. <https://doi.org/10.1111/j.1399-5618.2012.01013.x>
- Mertens J, Wang Q, Kim Y, Yu DX, Pham S, Yang B, et al. Differential responses to lithium in hyperexcitable neurons from patients with bipolar disorder. *Nature*. 2015;527:95–99. <https://doi.org/10.1038/nature15526>
- Stern S, Santos R, Marchetto MC, Mendes APD, Rouleau GA, Biesmans S, et al. Neurons derived from patients with bipolar disorder divide into intrinsically different sub-populations of neurons, predicting the patients' responsiveness to lithium. *Mol Psychiatry*. 2018;23:1453–65. <https://doi.org/10.1038/mp.2016.260>
- Stern S, Sarkar A, Stern T, Mei A, Mendes APD, Stern Y, et al. Mechanisms underlying the hyperexcitability of CA3 and dentate gyrus hippocampal neurons derived from patients with bipolar disorder. *Biol Psychiatry*. 2020;88:139–49. <https://doi.org/10.1016/j.biopsych.2019.09.018>
- Stern S, Sarkar A, Galor D, Stern T, Mei A, Stern Y, et al. A physiological instability displayed in hippocampal neurons derived from lithium-nonresponsive bipolar disorder patients. *Biol Psychiatry*. 2020;88:150–8. <https://doi.org/10.1016/j.biopsych.2020.01.020>
- Wigström H. A model of a neural network with recurrent inhibition. *Kybernetik*. 1974;16:103–12. <https://doi.org/10.1007/BF00271633>
- Espinoza C, Guzman SJ, Zhang X, Jonas P. Parvalbumin+ interneurons obey unique connectivity rules and establish a powerful lateral-inhibition microcircuit in dentate gyrus. *Nat Commun*. 2018;9:4605. <https://doi.org/10.1038/s41467-018-06899-3>
- Engin E, Zarnowska ED, Benke D, Tsvetkov E, Sigal M, Keist R, et al. Tonic inhibitory control of dentate gyrus granule cells by $\alpha 5$ -containing GABAA receptors reduces memory interference. *J Neurosci*. 2015;35:13698–712. <https://doi.org/10.1523/JNEUROSCI.1370-15.2015>
- Guzman SJ, Schlögl A, Espinoza C, Zhang X, Suter BA, Jonas P. How connectivity rules and synaptic properties shape the efficacy of pattern separation in the entorhinal cortex–dentate gyrus–CA3 network. *Nat Comput Sci*. 2021;1:830–42. <https://doi.org/10.1038/s43588-021-00157-1>
- Neunuebel JP, Knierim JJ. Spatial firing correlates of physiologically distinct cell types of the rat dentate gyrus. *J Neurosci*. 2012;32:3848–58. <https://doi.org/10.1523/JNEUROSCI.6038-11.2012>
- Neunuebel JP, Knierim JJ. CA3 retrieves coherent representations from degraded input: direct evidence for CA3 pattern completion and dentate gyrus pattern separation. *Neuron*. 2014;81:416–27. <https://doi.org/10.1016/j.neuron.2013.11.017>
- Madar AD, Ewell LA, Jones MV. Temporal pattern separation in hippocampal neurons through multiplexed neural codes. *PLOS Comput Biol*. 2019;15:e1006932. <https://doi.org/10.1371/journal.pcbi.1006932>
- Madar AD, Ewell LA, Jones MV. Pattern separation of spiketrains in hippocampal neurons. *Sci Rep*. 2019;9:5282. <https://doi.org/10.1038/s41598-019-41503-8>

37. Singh S, Becker S, Trappenberg T, Nunes A. Granule cells perform frequency-dependent pattern separation in a computational model of the dentate gyrus. *Hippocampus*. 2023;34:hipo.23585. <https://doi.org/10.1002/hipo.23585>
38. Berron D, Schutze H, Maass A, Cardenas-Blanco A, Kuijff HJ, Kumaran D, et al. Strong evidence for pattern separation in human dentate gyrus. *J Neurosci*. 2016;36:7569–79. <https://doi.org/10.1523/JNEUROSCI.0518-16.2016>
39. Santoro A. Reassessing pattern separation in the dentate gyrus. *Front Behav Neurosci*. 2013;7:96.
40. Madanlal D, Guinard C, Nuñez VP, Becker S, Garnham J, Khayachi A, et al. A pilot study examining the impact of lithium treatment and responsiveness on mnemonic discrimination in bipolar disorder. *J Affect Disord*. 2024;351:49–57. <https://doi.org/10.1016/j.jad.2024.01.146>
41. Khayachi A, Abuzgaya M, Liu Y, Jiao C, Dejjgaard K, Schorova L, et al. Akt and AMPK activators rescue hyperexcitability in neurons from patients with bipolar disorder. *EBioMedicine*. 2024;104:105161. <https://doi.org/10.1016/j.ebiom.2024.105161>
42. Aradi I, Holmes WR. Role of multiple calcium and calcium-dependent conductances in regulation of hippocampal dentate granule cell excitability. *J Comput Neurosci*. 1999;6:215–35.
43. Yim MY, Hanuschkin A, Wolfart J. Intrinsic rescaling of granule cells restores pattern separation ability of a dentate gyrus network model during epileptic hyperexcitability. *Hippocampus*. 2015;25:297–308. <https://doi.org/10.1002/hipo.22373>
44. Santhakumar V, Aradi I, Soltesz I. Role of mossy fiber sprouting and mossy cell loss in hyperexcitability: a network model of the dentate gyrus incorporating cell types and axonal topography. *J Neurophysiol*. 2005;93:437–53. <https://doi.org/10.1152/jn.00777.2004>
45. Carnevale NT, Hines ML. *The NEURON book*. Cambridge University Press; United Kingdom 2006.
46. Kochenderfer MJ, Wheeler TA. *Algorithms for optimization*. The MIT Press; Cambridge, Massachusetts, USA 2019.
47. Myers CE, Scharfman HE. A role for hilar cells in pattern separation in the dentate gyrus: a computational approach. *Hippocampus*. 2009;19:321–37. <https://doi.org/10.1002/hipo.20516>
48. Bates D, Mächler M, Bolker B, Walker S. Fitting linear mixed-effects models using lme4. *J Stat Softw*. 2015;67:1–48. <https://doi.org/10.18637/jss.v067.i01>
49. Treves A, Rolls ET. Computational analysis of the role of the hippocampus in memory. *Hippocampus*. 1994;4:374–91. <https://doi.org/10.1002/hipo.450040319>
50. O'Reilly RC, McClelland JL. Hippocampal conjunctive encoding, storage, and recall: avoiding a trade-off. *Hippocampus*. 1994;4:661–82. <https://doi.org/10.1002/hipo.450040605>
51. Kanerva P. *Sparse distributed memory*. The MIT Press; Cambridge, Massachusetts, USA. 2003.
52. Chavlis S, Petrantonakis PC, Poirazi P. Dendrites of dentate gyrus granule cells contribute to pattern separation by controlling sparsity. *Hippocampus*. 2017;27:89–110. <https://doi.org/10.1002/hipo.22675>
53. Kim S-Y, Lim W. Dynamical origin for winner-take-all competition in a biological network of the hippocampal dentate gyrus. *Phys Rev E*. 2022;105:014418. <https://doi.org/10.1103/PhysRevE.105.014418>
54. GoodSmith D, Chen X, Wang C, Kim SH, Song H, Burgalossi A, et al. Spatial representations of granule cells and mossy cells of the dentate gyrus. *Neuron*. 2017;93:677–90.e5. <https://doi.org/10.1016/j.neuron.2016.12.026>
55. Danielson NB, Turi GF, Ladow M, Chavlis S, Petrantonakis PC, Poirazi P, et al. In vivo imaging of dentate gyrus mossy cells in behaving mice. *Neuron*. 2017;93:552–9.e4. <https://doi.org/10.1016/j.neuron.2016.12.019>
56. Ben-Ari Y, Gaiarsa J-L, Tyzio R, Khazipov R. GABA: a pioneer transmitter that excites immature neurons and generates primitive oscillations. *Physiol Rev*. 2007;87:1215–84. <https://doi.org/10.1152/physrev.00017.2006>
57. Sipilä ST, Huttu K, Voipio J, Kaila K. Intrinsic bursting of immature CA3 pyramidal neurons and consequent giant depolarizing potentials are driven by a persistent Na^+ current and terminated by a slow Ca^{2+} -activated K^+ current. *Eur J Neurosci*. 2006;23:2330–8. <https://doi.org/10.1111/j.1460-9568.2006.04757.x>
58. Kerschensteiner D. Spontaneous network activity and synaptic development. *Neuroscientist*. 2014;20:272–90. <https://doi.org/10.1177/1073858413510044>
59. Blankenship AG, Feller MB. Mechanisms underlying spontaneous patterned activity in developing neural circuits. *Nat Rev Neurosci*. 2010;11:18–29. <https://doi.org/10.1038/nrn2759>
60. Sun H, Yan R, Hua L, Xia Y, Chen Z, Huang Y, et al. Abnormal stability of spontaneous neuronal activity as a predictor of diagnosis conversion from major depressive disorder to bipolar disorder. *J Psychiatr Res*. 2024;171:60–68. <https://doi.org/10.1016/j.jpsychires.2024.01.028>
61. Fountoulakis KN, Vieta E, Bouras C, Notaridis G, Giannakopoulos P, et al. A systematic review of existing data on long-term lithium therapy: neuroprotective or neurotoxic? *Int J Neuropsychopharmacol*. 2008;11:269–87. <https://doi.org/10.1017/S1461145707007821>
62. Honig A, Arts BMG, Ponds RWHM, Riedel WJ. Lithium induced cognitive side-effects in bipolar disorder: a qualitative analysis and implications for daily practice. *Int Clin Psychopharmacol*. 1999;14:167.
63. Burdick KE, Millett CE, Russo M, Alda M, Alliey-Rodriguez N, Anand A, et al. The association between lithium use and neurocognitive performance in patients with bipolar disorder. *Neuropsychopharmacology*. 2020;45:1743–9. <https://doi.org/10.1038/s41386-020-0683-2>
64. Cipriani A, Pretty H, Hawton K, Geddes JR. Lithium in the prevention of suicidal behavior and all-cause mortality in patients with mood disorders: a systematic review of randomized trials. *Am J Psychiatry*. 2005;162:1805–19. <https://doi.org/10.1176/appi.ajp.162.10.1805>
65. BALANCE investigators and collaborators, Geddes JR, Goodwin GM, Rendell J, Azorin J, Cipriani A, et al. Lithium plus valproate combination therapy versus monotherapy for relapse prevention in bipolar I disorder (BALANCE): a randomised open-label trial. *Lancet*. 2010;375:385–95. [https://doi.org/10.1016/S0140-6736\(09\)61828-6](https://doi.org/10.1016/S0140-6736(09)61828-6)
66. Baker S, Vieweg P, Gao F, Gilboa A, Wolbers T, Black SE, et al. The human dentate gyrus plays a necessary role in discriminating new memories. *Curr Biol*. 2016;26:2629–34. <https://doi.org/10.1016/j.cub.2016.07.081>
67. Chen G, Rajkowska G, Du F, Seraji-Bozorgzad N, Manji HK. Enhancement of hippocampal neurogenesis by lithium. *J Neurochem*. 2000;75:1729–34. <https://doi.org/10.1046/j.1471-4159.2000.0751729.x>
68. Palmos AB, Duarte RRR, Smeeth DM, Hedges EC, Nixon DF, Thuret S, et al. Lithium treatment and human hippocampal neurogenesis. *Transl Psychiatry*. 2021;11:1–8. <https://doi.org/10.1038/s41398-021-01695-y>
69. Swan AA, Clutton JA, Chary PK, Cook SG, Liu GG, Drew MR. Characterization of the role of adult neurogenesis in touch-screen discrimination learning: Neurogenesis and discrimination learning. *Hippocampus*. 2014;24:1581–91. <https://doi.org/10.1002/hipo.22337>
70. Tronel S, Beldou L, Grosjean N, Revest J, Piazza P, Koehl M, et al. Adult-born neurons are necessary for extended contextual discrimination. *Hippocampus*. 2012;22:292–8. <https://doi.org/10.1002/hipo.20895>
71. Luu P, Sill OC, Gao L, Becker S, Wojtowicz JM, Smith DM. The role of adult hippocampal neurogenesis in reducing interference. *Behav Neurosci*. 2012;126:381–91. <https://doi.org/10.1037/a0028252>
72. Nunes A, Singh S, Allman J, Becker S, Ortiz A, Trappenberg T, et al. A critical evaluation of dynamical systems models of bipolar disorder. *Transl Psychiatry*. 2022;12:416. <https://doi.org/10.1038/s41398-022-02194-4>
73. Sunkin S. Cell types database documentation: electrophysiology overview [white paper]. Allen Institute. 2017. <https://community.brain-map.org/uploads/short-url/veJ9z4lwAJoxv4Rx23b7KpnUYEp.pdf>.
74. Marin-Burgin A, Mongiat LA, Pardi MB, Schinder AF. Unique processing during a period of high excitation/inhibition balance in adult-born neurons. *Science*. 2012;335:1238–42. <https://doi.org/10.1126/science.1214956>
75. Groisman AI, Yang SM, Schinder AF. Differential coupling of adult-born granule cells to parvalbumin and somatostatin interneurons. *Cell Rep*. 2020;30:202–14.e4. <https://doi.org/10.1016/j.celrep.2019.12.005>
76. Temprana SG, Mongiat LA, Yang SM, Trinchero MF, Alvarez DD, Kropff E, et al. Delayed coupling to feedback inhibition during a critical period for the integration of adult-born granule cells. *Neuron*. 2015;85:116–30. <https://doi.org/10.1016/j.neuron.2014.11.023>
77. Toni N, Schinder AF. Maturation and functional integration of new granule cells into the adult hippocampus. *Cold Spring Harb Perspect Biol*. 2016;8:a018903. <https://doi.org/10.1101/cshperspect.a018903>
78. Finnegan R, Becker S. Neurogenesis paradoxically decreases both pattern separation and memory interference. *Front Syst Neurosci*. 2015;9:136. <https://doi.org/10.3389/fnsys.2015.00136>
79. Williams R, Ryves WJ, Dalton EC, Eickholt B, Shaltiel G, Agam G, et al. A molecular cell biology of lithium. *Biochem Soc Trans*. 2004;32:799–802. <https://doi.org/10.1042/BST0320799>
80. Kim HJ, Thayer SA. Lithium increases synapse formation between hippocampal neurons by depleting phosphoinositides. *Mol Pharmacol*. 2009;75:1021–30. <https://doi.org/10.1124/mol.108.052357>
81. McClelland JL, McNaughton BL, O'Reilly RC. Why there are complementary learning systems in the hippocampus and neocortex: insights from the successes and failures of connectionist models of learning and memory. *Psychol Rev*. 1995;102:419–57. <https://doi.org/10.1037/0033-295X.102.3.419>
82. Borzello M, Ramirez S, Treves A, Lee I, Scharfman H, Stark C, et al. Assessments of dentate gyrus function: discoveries and debates. *Nat Rev Neurosci*. 2023;24:502–17. <https://doi.org/10.1038/s41583-023-00710-z>

ACKNOWLEDGEMENTS

This research was supported by Research Nova Scotia (Abraham Nunes), an Ontario Graduate Scholarship (Selena Singh), and the Zuckerman STEM leadership program (Shani Stern). Fig. 1 was created using biorender.com.

AUTHOR CONTRIBUTIONS

Selena Singh contributed to the conceptualization, methodology, and software development, performed formal analyses, data curation and visualization, writing the original draft and subsequent revisions. Anouar Khayachi and Martin Alda provided access to data (resources) and contributed to manuscript editing and review. Shani Stern and Thomas Trappenberg contributed to manuscript editing and review. Abraham Nunes contributed to the conceptualization, methodology and software development, visualization, access to data (resources), writing the original draft, editing and review, supervision, project administration and funding acquisition.

COMPETING INTERESTS

The authors declare no competing interests.

ADDITIONAL INFORMATION

Supplementary information The online version contains supplementary material available at <https://doi.org/10.1038/s41398-025-03559-1>.

Correspondence and requests for materials should be addressed to Abraham Nunes.

Reprints and permission information is available at <http://www.nature.com/reprints>

Publisher's note Springer Nature remains neutral with regard to jurisdictional claims in published maps and institutional affiliations.



Open Access This article is licensed under a Creative Commons Attribution-NonCommercial-NoDerivatives 4.0 International License, which permits any non-commercial use, sharing, distribution and reproduction in any medium or format, as long as you give appropriate credit to the original author(s) and the source, provide a link to the Creative Commons licence, and indicate if you modified the licensed material. You do not have permission under this licence to share adapted material derived from this article or parts of it. The images or other third party material in this article are included in the article's Creative Commons licence, unless indicated otherwise in a credit line to the material. If material is not included in the article's Creative Commons licence and your intended use is not permitted by statutory regulation or exceeds the permitted use, you will need to obtain permission directly from the copyright holder. To view a copy of this licence, visit <http://creativecommons.org/licenses/by-nc-nd/4.0/>.

© The Author(s) 2025